Academic Open Internet Journal www.acadjournal.com Volume 21, 2007
ISSN 1311-4360

CONVECTIVE DIFFUSION PROCESS OF BLOOD VESSELS IN THE PRESENCE OF POROUS EFFECTS

Anil Kumar
Department of Mathematics
Dr. K. N. Modi Institute of Engineering & Technology,
Modinagar-201204, Ghaziabad (India)
drkumaranil73@yahoo.co.in

ABSTRACT

In this paper, convective dominated diffusion process in an axi-symmetric tube with a local constriction simulating a stenosed artery considering the porosity effects is carried out. The investigations demonstrate the effects of wall shear stress and recirculating flow on the concentration distribution in the vessels lumen and on wall mass transfer keeping the porosity in view. The flow is governed by the incompressible Navier-Stokes equations for Newtonian fluid in porous effects. The convection diffusion equation is used for the mass transport. The effect of porosity is examined on the velocity field and wall shear stress. The numerical solutions of the flow equations and the coupled mass transport equations are solved using finite difference scheme. The study explains the effect of porosity of the flow on the mass transport. The works that consider the possibility of reducing these flow instabilities using porous effect are reviewed.

Key words: Blood Vessels, Porosity, Wall Shear Stress, Simulation, Convection Diffusion

1. INTRODUCTION

Computational fluid dynamics simulations of complex flows in vascular passages such as cerebral or carotid arteries can provide clinicians with information needed to evaluate how pathologies from, how they evolve and ultimately how they are effectively treated. The geometry of blood vessels and arterial wall, their structure and mechanical properties depend on the pressure and flow conditions. In general stenosed arteries respond to sustained change in pressure of flow with remodeling functional characteristics of the artery. The porosity effects on blood flow cannot be ignored while studying a realistic problem. Some of the studies on the arterial flows are given as follows. Analytical transport phenomena are important to the understanding of vascular diseases is established by Fry and Vaishnav (1980).

Liepsch and Moravec (1984) investigated the flow of a shear thining blood, analog fluid in pulsatile flow through arterial branch model and observed large differences in velocity profiles relative to these measured with Newtonian fluids having the high shear rate viscosity of the analog fluid. Rodkiewicz et al. (1990) used several different non-Newtonian models for simulations of blood flow in large arteries and they observed that there is no effect of the yield stress of blood on either the velocity profiles or the wall shear stress. Out of these a large number of numerical studies concentrate on the transport phenomena in the microcirculation. Bassingthwaitghte et al. (1992) studied the exchange of gases between the systemic capillaries and the surrounding tissue. Very much attention has not been given to the numerical investigation of transport phenomena in large arteries keeping porosity in view.

The reason for this may be that most of these phenomena are highly convection dominated due to the low diffusion coefficients in quite a large

number of cases. In the arterial system there is evidence that fluid dynamic factors, especially shear forces, affect blood phase transport as well as properties of the vascular wall like wall permeability to solutes of gases [Tarbell (1993)]. Cavalcanti (1995) has discussed the inadequacies of such studies for the determination of the model for plaque growth. These observations provide future direction for research. Back et al. (1996) founded the important hemo-dynamical characteristics like the wall shear stress, pressure drop and frictional resistance in catheterized coronary arteries under normal as well as the pathological conditions due to stenosis being present. Rapptisch and Perktold (1996) investigated computer simulations of convective diffusion process in large arteries. For heat transfer in muscle tissues, Weinbaun et al. (1997) found that a correction factor of efficiency needs to be multiplied by the perfusion source term in the Pennes equation for bio heat transfer in a muscle tissue. This coefficient is a function of vascular cross-section geometry and is independent of the Peclet number

Korenga et al. (1998) consider a biochemical factors such as gene expression and albumin transport in atherogenessis and in plaque rupture. These have been shown to activate by hemo-dynamic factors in wall shear stress. However the concept of suction by tissues present in the vessels has not been considered in these studies. Rachev et al. (1998) have considered a model for geometric and mechanical adaptation of arteries. Lei et al. (1998) investigated a complex model for the transvascular exchange and extravascular transport of both fluid and macromolecules in a spherical solid tumor, the micro vascular lymphatic and tissue space were each considered as a porous medium. Tang et al. (1999) analysed blood flow in carotid arteries with stenosis.

Berger and Jou (2000) measured wall shear stress down stream of axi-symmetric stenoses in the presence of hemo-dynamics forces acting on the plaque, which may be responsible for plaque rupture. Stroud et al. (2000) founded the influence of stenosis morphology on flow fields and on quantities such as wall shear stress among stenotic vessels with very mild stenosis. Sharma et al. (2001) considered a mathematical analysis of blood flow through arteries using finite element Galerkin approaches. Tada and Tarbell (2000) utilized the Brinkman model to investigate the two-dimensional interstitial flow through the tunica media of an artery wall in the presence of an internal elastic lamina. Sharma et al. (2001) profounded MHD flow in stenosed artery using finite difference technique. Khaled and Vafai (2003) studied flow and heat transport in porous media using mass diffusion and different convective flow models such as Darcy and the Brinkman models, Energy transport in tissue is also analysed.

In the present study the steady convective diffusion of oxygen in an axi-symmetric tube with a local constriction simulating a stenosed blood vessel is investigated numerically applying a passive transport law for the flow of and mass transfer parameter with effect of porous to take account of wall porosity. An important aspect of this analysis is the comparison of two models for the solute wall flux one is assuming constant wall permeability and the second incorporating shear dependant wall permeability in the presence of porosity. This work was motivated by the study of lateral dispersion of cholesterol in arteries, where the blood containing cholesterol flows through and past the porous medium [Shivkumar (2001)]. Sharma et al. (2004) studied performance

modeling and analysis of blood flow in elastic arteries. Kumar et al. (2005) studied computational technique for flow in blood vessels with porous effects.

2. Formulation of the Problem:

In the present investigation the flow formulation for Navier-Stokes equations for incompressible Newtonian fluids in the porous effect has been considered. For an axi-symmetric coordinate (z, r) the equations can be written as:

$$\frac{\partial u}{\partial t}+u\frac{\partial u}{\partial z}+v\frac{\partial u}{\partial r}=-\frac{1}{\rho}\frac{\partial u}{\partial z}+\nu\left(\frac{\partial^2 u}{\partial z^2}+\frac{\partial^2 u}{\partial r^2}+\frac{1}{r}\frac{\partial u}{\partial r}\right)-\nu\frac{u}{k}, \tag{1}$$

$$\frac{\partial v}{\partial t}+u\frac{\partial v}{\partial z}+v\frac{\partial v}{\partial r}=-\frac{1}{\rho}\frac{\partial v}{\partial r}+\nu\left(\frac{\partial^2 v}{\partial z^2}+\frac{\partial^2 v}{\partial r^2}+\frac{1}{r}\frac{\partial v}{\partial r}-\frac{v}{r^2}\right)-\nu\frac{v}{k} \tag{2}$$

$$\frac{\partial u}{\partial z}+\frac{\partial v}{\partial r}+\frac{v}{r}=0 \tag{3}$$

where u and v are the axial (z) and radial (r) velocity components, ρ is the constant fluid density, p is the fluid pressure and ν is kinematic coefficient of viscosity.

The stream function –viscosity form of the Navier-Stokes equation has a major advantage over the primitive variable from in two-dimensional incompressible flow problem so far as numerical solutions of these equations are concerned.

Here

$$u=\frac{1}{r}\frac{\partial \psi}{\partial r}, v=-\frac{1}{r}\frac{\partial \psi}{\partial z}.$$

and vorticity is

$$\zeta = \frac{\partial v}{\partial z} - \frac{\partial u}{\partial r}. \tag{4}$$

The equations (3) can be written as,

$$\frac{\partial^2 \psi}{\partial z^2} + \frac{\partial^2 \psi}{\partial r^2} + \zeta r = \frac{1}{r}\frac{\partial \psi}{\partial r}, \tag{5}$$

$$\frac{\partial \zeta}{\partial t} + \frac{1}{r}\left(\frac{\partial \psi}{\partial r}\frac{\partial \zeta}{\partial z} - \frac{\partial \psi}{\partial z}\frac{\partial \zeta}{\partial r}\right) + \frac{\zeta}{r^2}\frac{\partial \psi}{\partial z} = \nu\left(\frac{\partial^2 \psi}{\partial z^2} + \frac{\partial^2 \psi}{\partial r^2} + \frac{1\partial \zeta}{r\partial r} + \frac{\zeta}{r^2} - \frac{1}{k}\zeta\right) \tag{6}$$

Taking the r-derivative of equation (1) and subtracting the z-derivative of equation (2), pressure term has been eliminated.

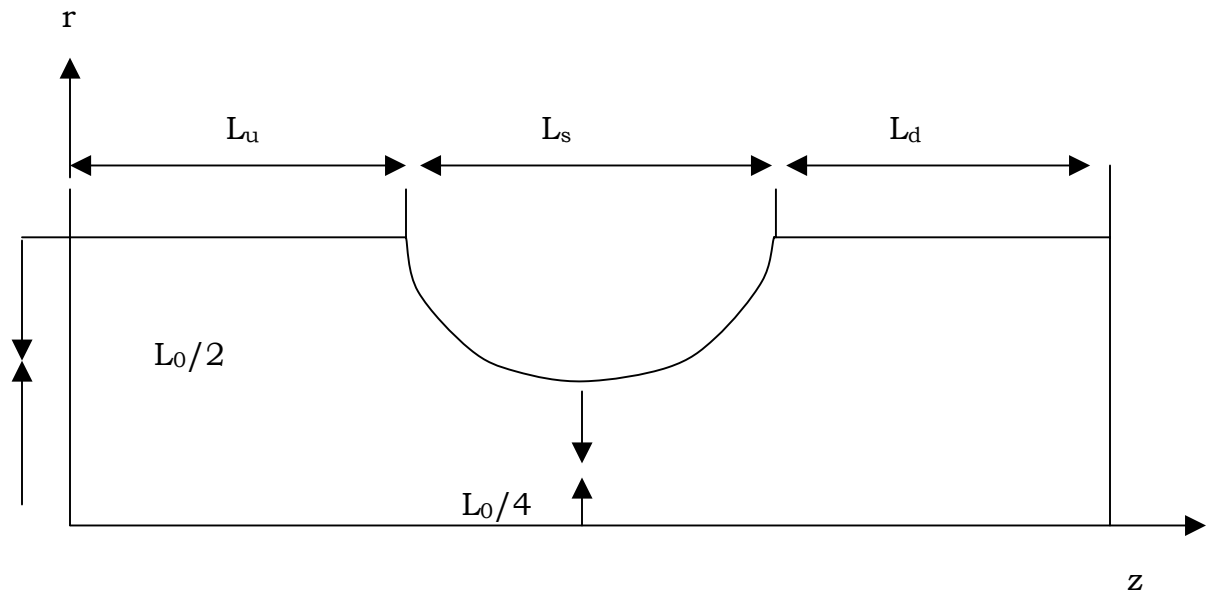

Figure 1. Geometrical construction of an artery segment with stenosis**.**

The mass transport, which is coupled to the velocity field, is modeled by the convection diffusion equation as given below:

$$\frac{\partial c}{\partial t} + u\frac{\partial c}{\partial z} + v\frac{\partial c}{\partial r} = D\left(\frac{\partial^2 c}{\partial z^2} + \frac{\partial^2 c}{\partial r^2} + \frac{1}{r}\frac{\partial c}{\partial r}\right), \tag{7}$$

where c denotes the solute concentration and D the constant diffusion coefficient. To make the parameters non –dimensional forms we put:

$$z^* = z/L_0 \qquad r^* = r/L_0 \qquad u^* = u/U_0,$$

$$v^* = v/U_0, \qquad c^* = c/C_0, \qquad t^* = tU_0/L_0 \tag{8}$$

The convective diffusion equation can be written in non-dimensional forms as:

$$\frac{\partial c^*}{\partial t^*} + u^* \frac{\partial c^*}{\partial z^*} + v^* \frac{\partial c^*}{\partial r^*} = \frac{1}{P_e}\left(\frac{\partial^2 c^*}{\partial z^{*2}} + \frac{\partial^2 c^*}{\partial r^{*2}} + \frac{1}{r^*}\frac{\partial c^*}{\partial r^*}\right), \tag{9}$$

where L_0 the reference length, U_0 the reference velocity and C_0 the reference concentration. Peclet number is defined as:

$$P_e = \frac{U_0 L_0}{D} = R_e S_c. \tag{10}$$

where $R_e = \dfrac{\rho U_0 L_0}{\mu}$ is Reynolds number and $Sc = \mu/\rho D$ is Schmidt number.

For the large Peclet number the hyperbolic part $u^* \dfrac{\partial c^*}{\partial z^*} + v^* \dfrac{\partial c^*}{\partial r^*}$, of the equation becomes dominant. The elliptic equations are used to generate the boundary fitted coordinate system. We are consider the following transformation.

$$\frac{\partial^2 \xi}{\partial z^2} + \frac{\partial^2 \xi}{\partial r^2} = 0, \frac{\partial^2 \eta}{\partial z^2} + \frac{\partial^2 \eta}{\partial r^2} = 0, \tag{11}$$

These equations constitute a transformation form the physical plane to numerical plane. This transformation is governed by the elliptic equation; it is called elliptic grid generation [Thompson (1974)]. The relations between the physical plane and the transformed plane are:

$$\frac{1}{J^2}\left(a^{11}\frac{\partial^2 z}{\partial \xi^2} - 2a^{12}\frac{\partial^2 z}{\partial \xi \partial \eta} + a^{22}\frac{\partial^2 z}{\partial \eta^2}\right) - \left(R\frac{\partial z}{\partial \xi} + S\frac{\partial z}{\partial \eta}\right) = 0, \tag{12}$$

$$\frac{1}{J^2}\left(a^{11}\frac{\partial^2 r}{\partial \xi^2}-2a^{12}\frac{\partial^2 r}{\partial \xi \partial \eta}+a^{22}\frac{\partial^2 r}{\partial \eta^2}\right)-\left(R\frac{\partial r}{\partial \xi}+S\frac{\partial z}{\partial \eta}\right)=0, \tag{13}$$

The metric coefficient and the Jacobian of the transformation are:

$$a^{11}=\frac{\partial^2 z}{\partial \eta^2}+\frac{\partial^2 r}{\partial \eta^2}, a^{12}=\frac{\partial^2 z}{\partial \xi^2}+\frac{\partial^2 r}{\partial \xi^2},\ a^{22}=\frac{\partial z}{\partial \xi}\frac{\partial z}{\partial \eta}+\frac{\partial r}{\partial \xi}\frac{\partial r}{\partial \eta}, J=\frac{\partial z}{\partial \xi}\frac{\partial r}{\partial \eta}-\frac{\partial z}{\partial \eta}\frac{\partial r}{\partial \xi},$$

The governing equations can be written as a coupled set of equations in terms of the stream function and vorticity as given below:

$$\frac{1}{J^2}\left(a^{11}\frac{\partial^2 \psi}{\partial \xi^2}-2a^{12}\frac{\partial^2 \psi}{\partial \xi \partial \eta}+a^{22}\frac{\partial^2 \psi}{\partial \eta^2}\right)-\left(R\frac{\partial \psi}{\partial \xi}+S\frac{\partial \psi}{\partial \eta}\right)+r\zeta=S_\psi, \tag{14}$$

$$\frac{\partial \zeta}{\partial t}+\frac{1}{r}\left(u^{\xi\eta}\frac{\partial \zeta}{\partial \xi}+v^{\xi\eta}\frac{\partial \zeta}{\partial \eta}\right)+\left[\frac{1}{J^2}\left(a^{11}\frac{\partial^2 \zeta}{\partial \xi^2}-2a^{12}\frac{\partial^2 \zeta}{\partial \xi \partial \eta}+a^{22}\frac{\partial^2 \zeta}{\partial \eta^2}\right)-\left(R\frac{\partial \zeta}{\partial \xi}+S\frac{\partial \zeta}{\partial \eta}\right)\right]=S_\zeta-K_\zeta,$$

(15)

where

$$u=\frac{1}{Jr}\left(-\frac{\partial z}{\partial \eta}\frac{\partial \psi}{\partial \xi}+\frac{\partial z}{\partial \xi}\frac{\partial \psi}{\partial \eta}\right), v=-\frac{1}{Jr}\left(\frac{\partial r}{\partial \eta}\frac{\partial \psi}{\partial \xi}-\frac{\partial r}{\partial \xi}\frac{\partial \psi}{\partial \eta}\right),$$

$$u^{\xi\eta}=\frac{1}{J}\left(u\frac{\partial r}{\partial \eta}-v\frac{\partial z}{\partial \eta}\right), v^{\xi\eta}=\frac{1}{J}\left(v\frac{\partial z}{\partial \eta}-u\frac{\partial r}{\partial \eta}\right), S_\psi=\frac{1}{Jr}\left(-\frac{\partial z}{\partial \eta}\frac{\partial \psi}{\partial \xi}+\frac{\partial z}{\partial \xi}\frac{\partial \psi}{\partial \eta}\right),$$

$$S_\zeta=\frac{1}{Jr}\left[\left(\frac{\partial r}{\partial \eta}\frac{\partial \psi}{\partial \xi}-\frac{\partial r}{\partial \xi}\frac{\partial \psi}{\partial \eta}\right)\zeta-v\left\{\left(-\frac{\partial z}{\partial \eta}\frac{\partial \zeta}{\partial \xi}+\frac{\partial z}{\partial \xi}\frac{\partial \zeta}{\partial \eta}\right)\right\}-\frac{\zeta}{r}+\frac{v\zeta}{r^2}\right],$$

$$K_\zeta=\frac{v}{Jr}\left(\left(-\frac{\partial z}{\partial \eta}\frac{\partial \psi}{\partial \xi}+\frac{\partial z}{\partial \xi}\frac{\partial \psi}{\partial \eta}\right)+\left(\frac{\partial r}{\partial \eta}\frac{\partial \psi}{\partial \xi}-\frac{\partial r}{\partial \xi}\frac{\partial \psi}{\partial \eta}\right)\right),$$

2.1 Boundary Conditions

Assuming a steady flow a fully developed parabolic velocity profile at the inlet are:

$$u(r) = 2U_0[1-(\frac{2r}{L_0})^2], z = 0, \quad (16)$$

at the wall a no slip condition is:

u = v = 0

and at axis of symmetry the normal velocity gradient is zero:

$$\nu = 0, \frac{\partial u}{\partial r} = 0, \frac{\partial \nu}{\partial r} = 0.$$

At the out flow boundary section zero surface traction force is assumed to be zero i.e.

$$-p\mathrm{n} + \mu \frac{\partial \mathrm{u}}{\partial \mathrm{n}} = 0,$$

where **n** is the outward unit normal vector and **u**=(u, v).

Evidently no slip conditions as given below:

$$\frac{\partial \psi}{\partial \mathrm{z}} = 0, \frac{\partial \zeta}{\partial \mathrm{z}} = 0 \text{ at } \xi = 1, \quad (17)$$

and $\psi = 0.5, \frac{\partial r}{\partial \eta}\frac{\partial \psi}{\partial \xi} + \frac{\partial r}{\partial \xi}\frac{\partial \psi}{\partial \eta} = 0$ at $\eta = 1,$

Following Rapptisch and Perktold (1996) the boundary conditions for the transport diffusive equations are constant concentration at the inlet,

c= C_0 , (18)

Zero axial concentration gradient $\frac{\partial c}{\partial \mathrm{z}} = 0$ at the outlet condition,

And for symmetry condition, $\frac{\partial c}{\partial r} = 0$,

For the diffusive flux at the wall, we consider the first model with constant wall permeability,

$$q_w = -D\frac{\partial c}{\partial n}\bigg|_{wall} = \alpha c_w, \tag{19}$$

where α is constant wall permeability and c_w is the wall concentration. And the other model permeability is dependent on the wall shear stress are given by,

$$q_w = -D\frac{\partial c}{\partial n}\bigg|_{wall} = g(|\tau_n|)c_n, \tag{20}$$

where $g(|\tau_n|)$ is the shear dependent wall permeability function.

3. Numerical Method

The spatially discrete from of the governing equations is obtained using a finite difference scheme.

The semi-discretized governing equations are written in the following from:

$$\frac{1}{j^2{}_{i.j}}\left(\frac{a_{i.j}{}^{11}}{\Delta\xi^2}D^{\xi} + D^{\xi} - \psi_{i.j} - \frac{a_{i.j}{}^{12}}{2\Delta\xi\Delta\eta}D^{\xi}{}_0 D^{\eta}{}_0\psi_{i.j} + \frac{a_{i.j}{}^{22}}{\Delta\eta^2}D^{\eta} + D^{\eta} - \psi_{i.j}\right)$$

$$- \left(\frac{R_{i.j}}{2\Delta\xi}D^{\xi}{}_0\psi_{i.j} + \frac{s_{i.j}}{2\Delta\eta}D^{\eta}{}_0\psi_{i.j}\right) + r_{i.j}\zeta_{i.j} = S_{\psi.j}, \tag{21}$$

$$\frac{\partial}{\partial t}\zeta_{i.j} + \frac{1}{r_{i,j}}\left(\frac{{}_u\xi\eta}{2\Delta\xi}D_0{}^{\xi}\zeta_{i.j} + \frac{{}_v\xi\eta}{2\Delta\eta}D_0{}^{\xi}\zeta_{i.j}\right)$$

$$\left[\frac{1}{j^2{}_{i.j}}\left(\frac{a^{11}{}_{i.j}}{\Delta\xi^2}D^{\xi}{}_{+}D^{\xi}\xi_{i.j} - \frac{ag^{12}{}_{i.j}}{2\Delta\xi\Delta\eta}D^{\xi}{}_0 D_0^{\eta}\xi_{i.j} + \frac{a^{22}{}_{i.j}}{\Delta\eta^2}D^{\eta}{}_{+}D_{-}^{\eta}\xi_{i.j}\right) - \left(\frac{R_{i.j}}{2\Delta\xi}D^{\xi}{}_0\xi_{i.j} + \frac{S_{i.j}}{2\Delta\eta}D^{\eta}\xi_{i.j}\right)\right]$$

$$= S_{\xi i.j} - K_{\xi i.j}, \tag{22}$$

for i=2,…m-1, j=2…,n-1.

The difference operators are defined as:

$$D_{+}^{\xi}F_{i.j} = F_{i+1.j} - F_{i.j}, D_{-}^{\xi}F_{i.j} = F_{i.j} - F_{i-1.j} and\ D_0F_{i.j} = F_{i+1.j} - F_{i-1.j}$$

Similarly $D_{+}^{\eta}f_{i.j} = f_{i.j+1} - f_{i.j}, D_{-}^{\eta}f_{i.j} = f_{i.j} - f_{i.j-1}$ and $D_0^{\eta}f_{i.j} = f_{i.j+1} - f_{i.j-1}$,

The discrete form of the boundary conditions given above can be obtained using the finite difference scheme.

$$\psi_{1,j} = r^2{}_{1,j}\left(1-\frac{1}{2}r^2{}_{1,j}\right), \zeta_{i.j} = -r_{1,j}, D^{\eta}{}_h r_{m.j} D^{\zeta}{}_h \psi_{m.j} D^{\eta}{}_h \psi_{m.j} = 0, \tag{23}$$

$$D^{\eta}{}_h r_{m.j} D^{\zeta}{}_h \zeta_{m.j} - D^{\zeta}{}_h r_{m.j} D^{\eta}{}_h \zeta_{m.j} = 0, \tag{24}$$

for J=2,…,n-1,

$$\psi_{i.1} = 0,\ \zeta_{i.j} = 0, \psi_{i.n} = 0.5,\quad D^{\eta}{}_h x_{i.n} D^{\xi}{}_h \psi_{i.n} + D^{\xi}{}_h x_{i.n} D^{\eta}{}_h \psi_{i.n} = 0, \tag{25}$$

for i=2,…,m-1,

where $D^{\xi}{}_h F_{i.j} = 3F_{i.j} - 4F_{i-1.j} + F_{i-2.j}, D^{\xi}{}_h F_{i.j} = -3F_{i.j} + 4F_{i+1.j} - F_{i+2.j}$,

and $D^{\eta}{}_h F_{i.j} = 3F_{i.j} - 4F_{i.j-1} + F_{i.j-2}$, (26)

while all the other boundary conditions are conventional, there is a computational difficulty with the no slip condition, since no vorticity value is available at the wall, j=n in order to solve the difference equations (22). For computation purpose, the following iterative algorithm is used following Huang et al. [1995]. This scheme is used for temporary discretization to ensure a second order accurate solution both in time and space for both convective and diffusion terms.

NUMERICAL ALGORITHM:

Step1. Solve equation (21) for j=2,…, n-1 and i=2,…, m-1. The stream function (ψ) at j=n-1 is calculated using both no slip boundary condition (17) at the wall. Gauss-Siedal method is used to solve the algebraic equations.

Step2. Update $\mu^{\xi\eta}$ and $v^{\xi\eta}$ using ψ from the previous step.

Step3. To calculate ζ at j =n-1 for i=1,..., m-1 use relation (21), coupling ψ and ζ, is satisfied at j=n-1;

Step4. Solve equation (22) at j=2,...,n-1 for i=2,...,m-1 using the value at j=n-1 from step (3) and necessary conditions at the other boundaries. Again using Gauss-Siedal method solves the algebraic equations.

Step5. Steps (1)-(4) are repeated until convergence is reached. The solution of convective diffusion equation can be obtained using the finite element technique following Rapptisch and Parktold(1996). The present algorithm is economic and efficient having a sharp convergence.

4. Results and Discussion

The simulation of the steady convective diffusion of dissolved oxygen in stenotic artery model has been performed and streamlines as well as continuous contour are given in figure 2(A) and 2(B). The simulation parameters for the flow and oxygen transport are such that the physiological conditions in the human abdominal aorta match with the same. The geometric parameters are taken as: inlet diameter L_0 =1.42 tube length upstream of the constriction diameter $L_0/2$=0.71 cm., length of the down stream domain L_d =65.5 cm. For the flow simulation and oxygen transport following parameters are applied: [Rappitsch and perktold (1996)], The simulation parameters are[Osenberg (1991)], mean flow rate =17.5 mls^{-1}, mean inlet velocity, U_0=10.52cms^{-1}. Kinemetic viscosity=0.333 poise.

The resulting Reynolds number R_e = 450, C_0 =$2.58\times10^{-3}$$mlcm^{-3}$, D =$1.6\times10^{-5}$ cm^2s^{-1} and reference wall flux

$g_0 = 4.82 \times 10^{-6}\, ml cm^{-2} s^{-1},\ \mathrm{P}_0 = 86 mm\mathrm{H}g, \lambda = 3.0 \times 10^{-5}\, ml$

$cm^{-3}\ \mathrm{mmH}g^{-1}\left(\mathrm{P}_0 = C_0 / \lambda\right)$. The Peclet number Pe =930000 indicate highly convection problem. The qualitative characteristic of the is concentration contours in the separated flow region shows sharp concentration gradient near the wall and the separating stream line are very similar to shape of the contours published by Ma et al. (1994) for mass transfer in sudden expansion tube model.

Figure 3(a) is drawn for the normalized mean cross sectional concentration. The comparison of the results with shear dependent wall permeability and constant wall permeability shown only slight difference. Figure 3 (b) depicts the main differences between the two permeability models occurring in the wall concentration. Figure 3(c) explains the non –dimensional diffusive wall flux. This study may have an important impact on the understanding of development of atherosclerotic diseases. The comparison of the result in the modal with constant wall permeability and in a model with shear dependent wall permeability demonstrates great differences in wall permeability. The results show that taking into account shear dependent permeability characteristics, depending on the special solute or gas, may have significant influence on the concentration distribution near and at the wall and consequently on the wall flux. The velocity profiles are shown in figure 4. Comparison between experimental and numerical simulation are made for the pressure distribution along the solid surface and the axial velocity profile.

5. Conclusion

Steady convective diffusion has studied on an axi-symmetric stenotic artery model in the presence of porous effect. The numerical solution of the flow equations is obtaining applying the finite differences scheme. The numerical result indicate strong dependence of oxygen transport to the wall in the geometric flow region by influencing the concentration boundary layer, which, depends on the local fluid mechanical shear. In the model with shear stress dependent permeability wall shear stress not only affects the concentration boundary layer, but also vascular permeability. In the shear dependent permeability model a second flux minimum occurred at the down stream end of the recirculation zone where wall shear stress and therefore wall permeability is slow. Numerical simulation of analytical stenosis offers a non-invasive means of obtaining detailed flow patterns associated with the disease. The effect of the porous medium is an elegant device for flow control. It is found that models for convective mass transport through porous media are widely applicable in the production of the osteoinductive material, simulation of blood flow of tumors and muscles and in modeling blood flow when fatty plagues of cholesterol and artery clogging clots and formal in the lumen.

Reference:

1. Beck, L. H; Kwack, E. Y; Back, M. R. (1996): Flow rate pressure drop relation in coronary angioplasty catheter obstruction effect, ASME, Journal of Biomechanical Engineering Transactions, 118, 83-89.
2. Bassingthwaitghte, J.B.; Deussen, A.; Beyer, D.; Chan, I.S.; Raymond, G.R.; King, R.B. Bukowski, T.R; Ploger, J.D; Kroll, K.; Revenaugh, J.; Link, J.M. and Krohin, K.A. (1992): Oxygen transport in the myocardium, Advanced Biological Heat and Mass Transfer ASME, 231, 113-119.

3. Berger, S.A. and Jou, L.D. (2000): Flows in stenotic vessels, Annual Review of fluid Mechanics, 32, 347-384.
4. Cavalcanti, S. (1995): Hemodynamics of an artery with mild stenosis , Journal of Biomechanics 28 , 387-399.
5. Fry, D.L. and Vaishnav, R.N. (1980): Mass transport in the arterial wall, In basic hemodynamics and its role in diseases processes, University park Press, Baltimore, 425-481.
6. Huang, H.; Modi, V.J. and Seymour (1995): Fluid mechanics of stenosed arteries, International Journal of Engineering Science, 33,6,815-828.
7. Khaled, A.R.A. and Vafai, K. (2003): The role of porous media in modeling flow and heat transfer in biological tissues, International Journal of Heat and Mass Transfer, 46, 4989-5003.
8. Korenga, R.; Ando, J. and Kamiya, A. (1998): The effect of laminar flow on the gene expression of the adhesion molecule in endothelial cells, Japanese Journal Medical Electronics and Biological Engineering 36, 266-272.
9. Kumar, Anil; Varshney, C.L. and Sharma, G.C. (2005): Computational technique fluid flow in blood vessels with porous effects, International Journal of Applied Mathematics and Mechanics (English Edition) China, 26, (1), 63-72.
10. Lei, X.X.; Wu, W. Y.; Wen, G.B. and Chen, J.G. (1998): Mass transport in solid tumors (I) fluid dynamics, Applied Mathematical Mechanics, (English Edition) 19, 1025-1032.
11. Liepsch, D. and Moravec, S. (1984): Pulsatile flow of non-Newtonian fluid in distensible models of human arteries, Biorheology, 21, 571-583.

12. Ma, P.J.; Li, X. and Ku, D.N. (1994): Heat and mass transfer in a separated flow region for high Prandtle and Schmidt numbers under pulsatile conditions, International Journal Heat and Mass Transfer 37, 2723-2736.
13. Osenberg, H.P. (1991): Simulation des artericllen blutflussen Ein Allgemeries modelmit anwendung axrf dasmenschliche Hirngen fabs system, dess ETH-Zurich 9442, IBT, Zurich.
14. Rachev, A.; Stergiopelos, N. and Meister, J.J. (1998): A model for geometric and mechanical adaptation of arteries to sustained hypertension, Journal of Bio-Mechanical Engineering, 120,9-17.
15. Rappitsch, G. and Perktold, K. (1996): Computer simulation of convective diffusion processes in large arteries, Journal of Bio-mechanics, 29, (2) 207-215.
16. Sharma, G.C.; Jain, M. and Kumar, Anil (2001): MHD flow in stenosed artery, Proceedings in International Conference on Mathematical Modeling, January 29-31, I.I.T. Roorkee, 683-687.
17. Sharma, G.C.; Jain, M. and Kumar, Anil (2001): Finite element Galerkin's approach for a computational study of arterial flow, International Journal of Applied Mathematical and Mechanics, China (English Edition), 22(9), 1012-1018.
18. Sharma G.C.; Jain, M. and Kumar, Anil. (2004): Performance modeling and analysis of blood flow in elastic arteries, International Journal of Mathematical and Computer Modelling, U.S.A., 39, 1491-1499.

19. Shivkumar, P. N. (2001): Mathematical modelling of some problem in industry and biology, Proceeding in International Conference on Mathematical Modeling, January 29-31, I.I.T. Roorkee, 601-604.
20. Stroud J.S., Berger, S. A. and Saloner, D.(2000): Influence of stenosis morphology on flow through severely stenotic vessels; implications for plaque rupture, Journal of Biomechanics, 33, 443-455.
21. Thompson, J.F.; Thomes, F.C. and Martin, C.W. (1974): Automatic numerical generation of body fitted curvilinear coordinate system for field containg any of arbitrary two-dimensional bodies, Journal of Computational Physics, 15, 299-319.
22. Tada, S. and Tarbell, J.M. (2000): Interstial flow through the internal elastic lamina affects shear stress on arterial smooth muscle cells, American Journal of Physiology, Heart Circulation Physiology, 278, (H, 1589-97).
23. Tang, D.; Yang, C.; Huang, Y. and Ku, D.N. (1999): Wall shear stress and strain analysis using a three-dimensional thick wall model with fluid-structure interactions for blood flow in carotid arteries with stenoses, Computers and Structures, 72, 341-377.
24. Tarbell, J.M. (1993): Bioengineering studies of the endothelial transport barrier, BMES- Bulletin, 17, 35-39.
25. Weinbaun, S.; Xu, L.X.; Zhu, L. and Expene, A. (1997): A new fundamental bioheat equation for muscle tissues blood perfusion terms, Journal of Biomechanical Engineering Transaction, ASME, (119), 278-288.

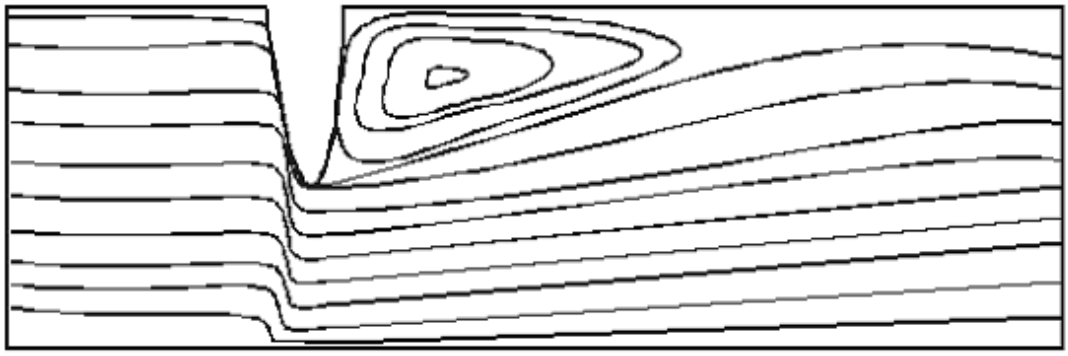

(A)

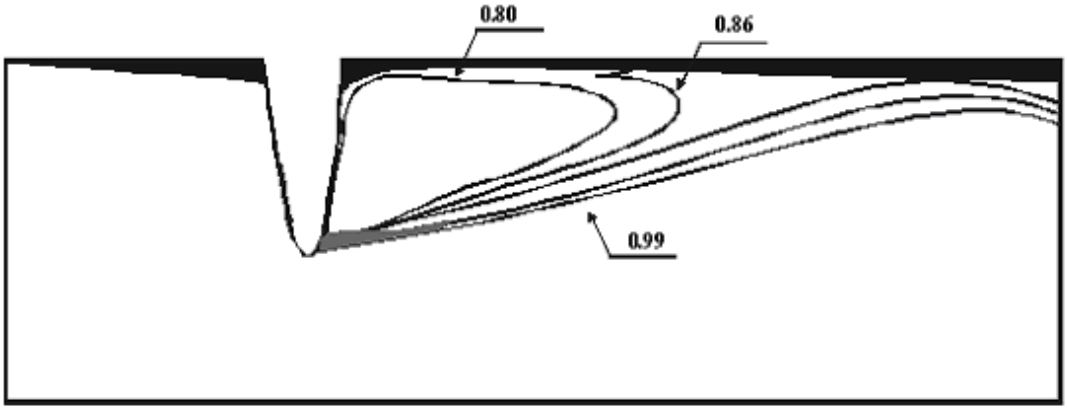

(B)

Fig. 2: Streamlines (A) and isoconcentration contours (B) for steady flow of Reynolds No.. 448 and Peclet. No.. 930000 in the presence of porous effects (ε=0.1). Numbers indicate normalized concentration values.

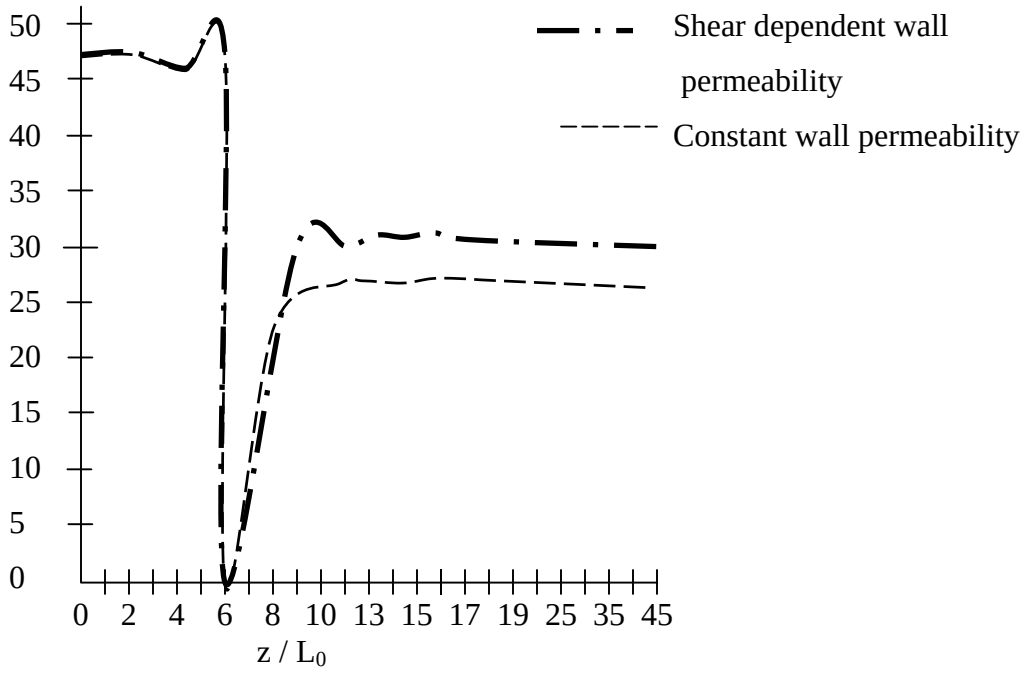

Fig.3 (a) Normalized mean cross sectional concentration

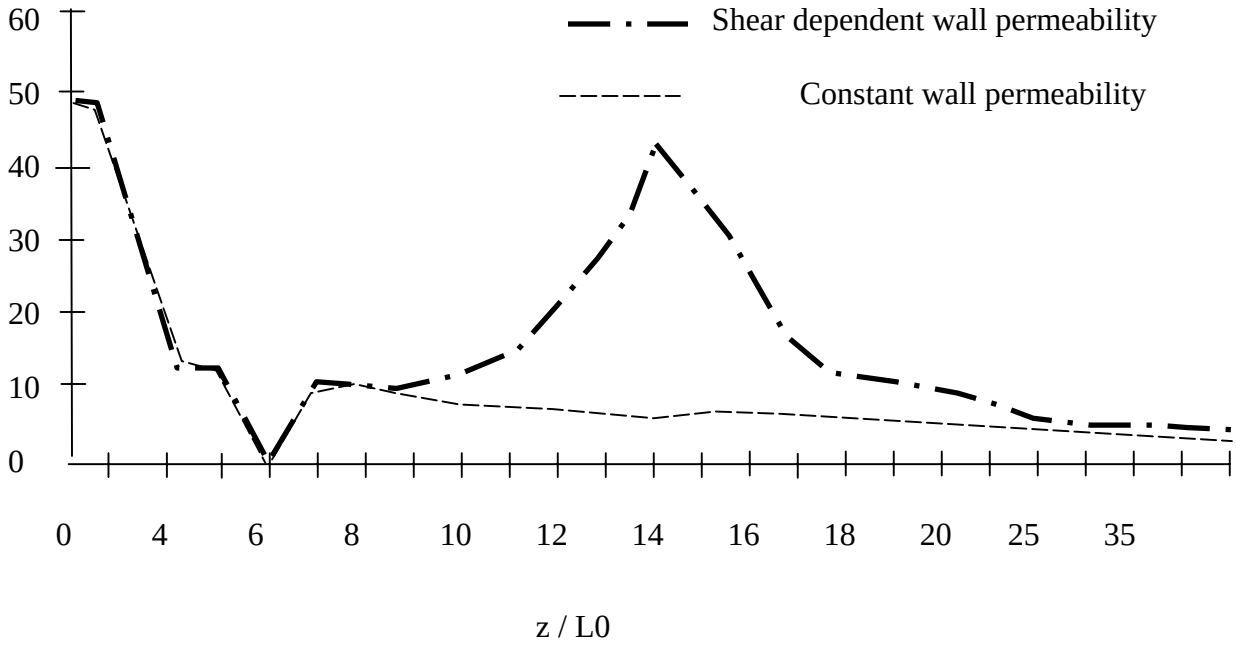

Figure 3 (b): Normalized wall concentration non-dimensional wall flux

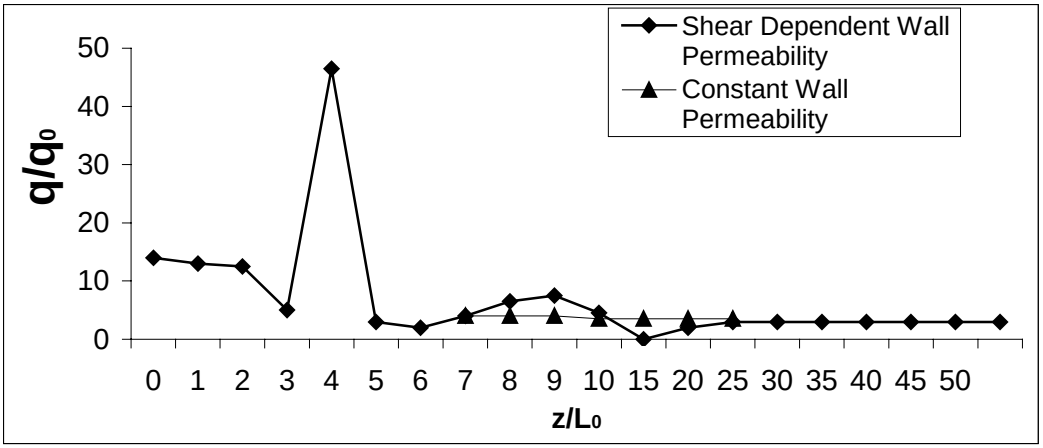

Figure 3 (c): Normalized Wall Concentration non-dimensional Diffusive flux.

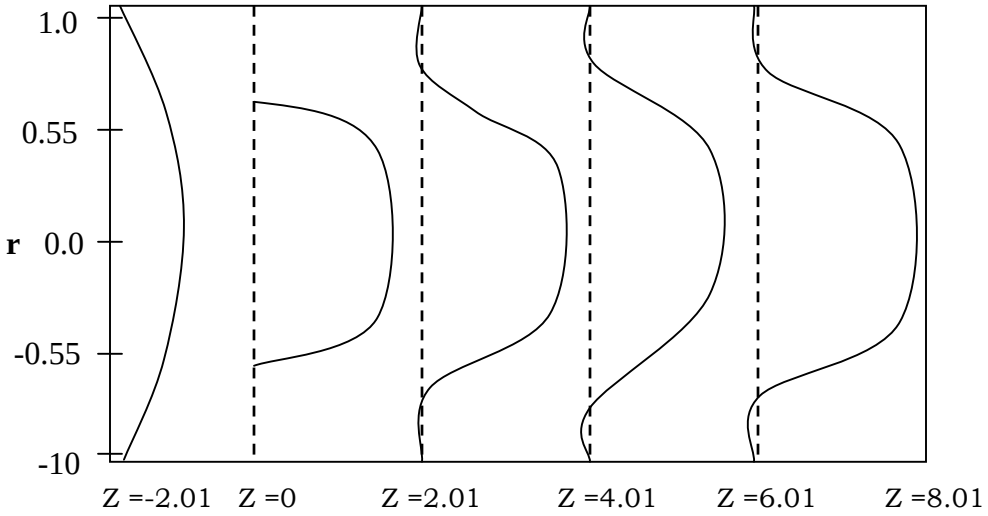

Figure 4 (a) Variation of axial velocity profile with porosity (K=0.1).

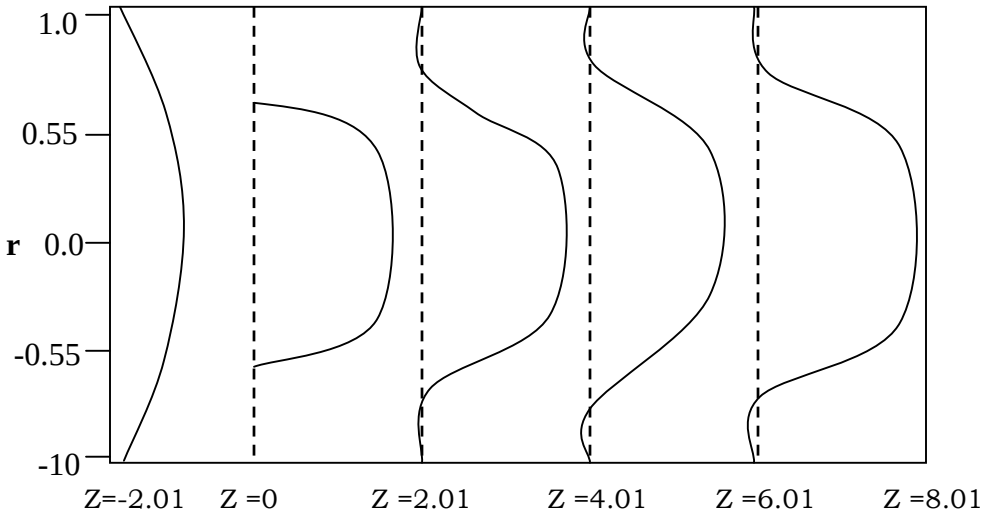

Figure 4 (b): Variation of axial velocity profile with porosity (K=0.2).